

# Study of $\text{LaSiO}_3\text{Cl}:\text{Ce}^{3+}, \text{Tb}^{3+}$ and $\text{Ca}_5\text{B}_2\text{SiO}_{10}:\text{Eu}^{3+}$ phosphors for improving hue standard and illuminating beam of WLEDs

Dieu An Nguyen Thi<sup>1</sup>, Phan Xuan Le<sup>2</sup>

<sup>1</sup>Faculty of Electrical Engineering Technology, Industrial University of Ho Chi Minh, Ho Chi Minh City, Viet Nam

<sup>2</sup>Faculty of Mechanical - Electrical and Computer Engineering, School of Engineering and Technology, Van Lang University, Ho Chi Minh City, Vietnam

---

## Article Info

### Article history:

Received Jul 23, 2021

Revised Sep 26, 2021

Accepted Dec 22, 2021

---

### Keyword:

WLEDs

$\text{LaSiO}_3\text{Cl}:\text{Ce}^{3+}, \text{Tb}^{3+}$

$\text{Ca}_5\text{B}_2\text{SiO}_{10}:\text{Eu}^{3+}$

Luminous efficacy

Color uniformity

Mie-scattering theory

---

## ABSTRACT

Remote phosphor arrangements usually have low color quality and superior lumen output to that of protective-coating phosphor arrangements and in-cup phosphor arrangements. For this reason, many researches are done so that we could enhance the chromatic quality for the remote phosphor arrangements. For this research, we are suggesting the double-layer remote phosphor arrangement to boost the CRI (short for color rendering index) as well as the CQS (short for color quality scale) in WLED devices. Three identical WLED arrangements which have dissimilar chromatic temperature which covers 5600 K, 8500 K will be utilized in this article. The initial idea involves placing one sheet of blue phosphor  $\text{LaSiO}_3\text{Cl}:\text{Ce}^{3+}, \text{Tb}^{3+}$  or one sheet of red phosphor  $\text{Ca}_5\text{B}_2\text{SiO}_{10}:\text{Eu}^{3+}$  above a sheet of yellow phosphor  $\text{YAG}:\text{Ce}^{3+}$ . Next, seek an appropriate concentration of  $\text{Ca}_5\text{B}_2\text{SiO}_{10}:\text{Eu}^{3+}$  so that we could obtain the most desirable chromatic performance. Judging the result, the element  $\text{Ca}_5\text{B}_2\text{SiO}_{10}:\text{Eu}^{3+}$  seem to help improve the CRI and CQS levels. Particularly, the more the concentration of  $\text{La}_2\text{O}_3:\text{Eu}^{3+}$  is the better level the CRI and the CQS will get, since there is the boost in red illumination within the WLED devices.

Copyright © 2022 Institute of Advanced Engineering and Science.  
All rights reserved.

---

## Corresponding Author:

Phan Xuan Le

Faculty of Mechanical - Electrical and Computer Engineering, School of Engineering and Technology,  
Van Lang University, Ho Chi Minh City, Vietnam

Email: le.px@vlu.edu.vn

---

## 1. INTRODUCTION

Clearly, the pc-WLEDs (stands for white-light diodes with conversion phosphor), and the conventional optical source which is replaced by the fourth potential generation, have countless applications in the optical field [1-3]. The said diodes are utilized in various fields such as street lighting systems, landscape, backlighting, etc. Nevertheless, it still faces some difficulties in the development process due to the effectiveness of optical extrication and the angular similarity for a CCT value (short for correlated color temperature) in the WLED device [4, 5]. It is necessary that certain development needs to be made to enhance the illumination effectiveness and hue standard, as there is a demanding market [6]. The composite including the illumination in blue color generated by the opposite phosphor in red color as well as LED chip's illumination in yellow color is the most popular method to produce the white light. Apparently, the configuration for the LEDs as well as the settlement concerning the phosphor sheets is vital for the establishment of lumen output, specifically the CRI [7, 8]. To create LEDs, there are some phosphor coating techniques such as conformal technique and dispensing technique [9-10]. However, they are not effective in improving color quality because the phosphor yellow emission causes the reduction in optical transmutation in phosphor elements to connect to the chip of LED. This causes the temperature boost between the LED device's connection and the sheet of phosphor. Hence, decreasing the heat emission will boost the capability of the phosphor as well as eliminate any impairment to the phosphor layer. The remote phosphor arrangement is introduced in some other researches that devide the sheet of phosphor from the LED chip to lower the impact

of the heat on it. This could help avoid backscattering and light circulation. This method, which is the optimal resolution to limit the heat emission of LED, is able to boost the lumen output and chromatic quality for the LED devices [11-16]. The remote phosphor arrangement is suitable for the standard lighting systems, however, it may not be sufficient for other lighting utilization. As such, we must introduce a new generation of LEDs. Some original remote phosphor arrangements are presented to diminish the scattering of the phosphor element aimed at the chip of LED as well as to enhance the lumen efficiency. An earlier analysis demonstrated that the remote phosphor layer with a reversed cone lens encapsulant along with a bordering band can turn the light emission from the chip of LED back to the LED device's exterior as well as decrease the depletion which is resulted from inverted reflection within the LED device [17]. One particular remote phosphor arrangement pattern having a visible area within the border which is not coating with phosphor can obtain higher consistency of correlated color temperature decided by angle as well as multi-colored consistency [18]. In addition, the underlayer sapphire for the remote phosphor formation can convey the better CCT level's consistency for a farther field formation compared to a standard formation [19]. The remote phosphor having a double-sheet arrangement seemingly has better optical emission quality in LEDs. The referred works mainly aim at boosting the chromatic homogeneity as well as the luminous flux emitting from WLED devices with the remote phosphor arrangement. These works also, however, merely concentrate on WLED devices having one chip and small chromatic temperature. Meanwhile, the improvement of WLEDs luminous flux with high color temperature is a complicated process. Additionally, there is no study that effectively compares the applications of different layouts of two phosphor sheets. Therefore, the LED producers find it difficult to pick the most desirable way so that they could boost the chromatic performance as well as the lumen emitting.

The paper's purpose is to recommend two structures of dual-layer remote phosphor arrangement so that we could enhance the chromatic performance of WLED devices in various chromatic temperatures ranging from 6600 K to 7700 K. The initial idea involves utilizing the sheet of  $\text{LaSiO}_3\text{Cl}:\text{Ce}^{3+}, \text{Tb}^{3+}$  phosphor in green color so that we could increase the green illumination portion within the WLED devices, causing the lumen boost. The next proposal involves utilizing a sheet of  $\text{Ca}_5\text{B}_2\text{SiO}_{10}:\text{Eu}^{3+}$  phosphor in red so that we could increase the red-illumination portion for WLED devices that later leads to the boost in CRI as well as CQS values. This article additionally explains in detail the chemical constituents in  $\text{Ca}_5\text{B}_2\text{SiO}_{10}:\text{Eu}^{3+}$  which directly affect the luminous attribute of WLEDs. From the result, CRI along with CQS values have been considerably boosted if the phosphor layer  $\text{Ca}_5\text{B}_2\text{SiO}_{10}:\text{Eu}^{3+}$  was added. Nevertheless, choosing an appropriate  $\text{LaSiO}_3\text{Cl}:\text{Ce}^{3+}, \text{Tb}^{3+}$  and  $\text{Ca}_5\text{B}_2\text{SiO}_{10}:\text{Eu}^{3+}$  concentration is needed to avoid the great loss of the chromatic performance as well as lumen output when the green or red phosphor concentration is higher than the required level. Three distinctions occur if one sheet of phosphor in red or green color is coated over the yellow phosphor layer  $\text{YAG}:\text{Ce}^{3+}$ . The initial difference is that the red or green light portion will cause a rise in the white illumination's emission spectra. Such an event becomes a key element for the color quality enhancement process. In addition, the light scattering as well as propagation for WLED devices appear to be reverse to the added concentration of phosphor. Thus, the selection for the desirable concentration of phosphor is very essential for sustaining the luminous flux for WLED devices.

## 2. RESEARCH METHOD

### 2.1. $\text{LaSiO}_3\text{Cl}:\text{Ce}^{3+}, \text{Tb}^{3+}$ and $\text{Ca}_5\text{B}_2\text{SiO}_{10}:\text{Eu}^{3+}$ granules: creation process

The  $\text{LaSiO}_3\text{Cl}:\text{Ce}^{3+}, \text{Tb}^{3+}$  particle is composed of  $\text{La}_2\text{O}_3$ ,  $\text{SiO}_2$ ,  $\text{CeO}_2$ ,  $\text{Tb}_4\text{O}_7$ ,  $\text{NH}_4\text{Cl}$ , see Table 1 and Table 2. The emission light of this phosphor is a pale shade of yellow and green color. The radiation highest point is 2.29 eV. The stimulation effectiveness by UV is ++ (4.88 eV), + (3.40 eV); QE is approximately 80-90%, and by e-beam is +/4%.

Table 1. Preparation of  $\text{LaSiO}_3\text{Cl}:\text{Ce}^{3+}, \text{Tb}^{3+}$

Step 1	Mix by stirring in water ( $\text{NH}_3$ develops)
Step 2	Let dry in air and powderize
Step 3	Fire ~1 hour, ~500°C in capped quartz tubes, $\text{N}_2$ . Powderize
Step 4	Fire 1 hour, 1200°C in capped quartz tubes, $\text{N}_2$ . Powderize
Step 5	Fire 1 hour, 1200°C within open quartz boats, CO. Powderize
Step 6	Wash several times in water then let dry in air.

Table 2. Ingredients of  $\text{LaSiO}_3\text{Cl}:\text{Ce}^{3+},\text{Tb}^{3+}$ 

Ingredients	Moles (%)	By weight (gram)
$\text{La}_2\text{O}_3$	100 (of La)	163
$\text{SiO}_2$	180	108
$\text{CeO}_2$	20	34
$\text{Tb}_4\text{O}_7$	14 (of Tb)	26
$\text{NH}_4\text{Cl}$	130	60

Phosphor  $\text{Ca}_5\text{B}_2\text{SiO}_{10}:\text{Eu}^{3+}$  composition includes four elements  $\text{CaCO}_3$ ,  $\text{H}_3\text{BO}_3$ ,  $\text{SiO}_2$ ,  $\text{Eu}_2\text{O}_3$ , see Table 3 and Table 4. The emission color is a red light. The emission peak is 2.03 eV. The stimulation effectiveness by UV is ++ (4.88 eV), - (3.40 eV); QE is about 50-60%, and by e-beam is poor.

Table 3. Preparation of  $\text{Ca}_5\text{B}_2\text{SiO}_{10}:\text{Eu}^{3+}$ 

Step 1	Mix by grinding or dry milling
Step 2	Fire 1 hour, 1100°C within open quartz boats, air. Powderize (milling)
Step 3	Fire 1 hour, 1200°C within open quartz boats, air. Powderize
Step 4	Fire 1 hour, 1300°C within open quartz boats, air.

Table 4. Ingredients of  $\text{Ca}_5\text{B}_2\text{SiO}_{10}:\text{Eu}^{3+}$ 

Ingredients	Moles (%)	By weight (gram)
$\text{CaCO}_3$	100	100
$\text{H}_3\text{BO}_3$	50	31
$\text{SiO}_2$	22	13.2
$\text{Eu}_2\text{O}_3$	5 (of Eu)	8.8

The chemical ingredients of  $\text{LaSiO}_3\text{Cl}:\text{Ce}^{3+},\text{Tb}^{3+}$  and  $\text{Ca}_5\text{B}_2\text{SiO}_{10}:\text{Eu}^{3+}$  are explained in detail shown by Table 1 and Table 2. The composition considerably affects the phosphor optical properties. Hence, before applying these particles to WLEDs, thoroughly studying their compositions is a must. The condition for these phosphors to be applied is the demand for a spectrum that is suitable to the blue illumination generated by the chip in the LED device. The spectrum which absorbs these phosphors has to be suited to the emission spectra in the blue chip. The absorption band in  $\text{LaSiO}_3\text{Cl}:\text{Ce}^{3+},\text{Tb}^{3+}$  under 250 nm - 502 nm is quite advantageous to absorb the illumination generated from various bands. As the blue illumination is not solely generated, the yellow illumination is generated as well through the conversion in the sheet of phosphor in yellow color. Identically,  $\text{Ca}_5\text{B}_2\text{SiO}_{10}:\text{Eu}^{3+}$  also has a large absorption band which is under 3.4 eV - 4.88 eV, with more than 70% in absorption efficacy. Before the optical simulation process for the  $\text{LaSiO}_3\text{Cl}:\text{Ce}^{3+},\text{Tb}^{3+}$  and  $\text{Ca}_5\text{B}_2\text{SiO}_{10}:\text{Eu}^{3+}$  particles, some numeric parameters have to be measured precisely including the concentration of phosphor, the granules' measurement of phosphor, excitation spectrum, absorption spectrum, as well as phosphor emission spectrum. In the listed factors, the concentration and the granules' measurement of phosphor would be elements that can maximize the color quality and the lumen output for the LED device. The other factors would be displayed as constant. Judging the result from the earlier study, the phosphor granules' diameter is kept firm at 14.5  $\mu\text{m}$ . Meanwhile,  $\text{LaSiO}_3\text{Cl}:\text{Ce}^{3+},\text{Tb}^{3+}$  and  $\text{Ca}_5\text{B}_2\text{SiO}_{10}:\text{Eu}^{3+}$  concentrations are modified so that we could pinpoint the best result which would be the main purpose of the research.

## 2.2. Building the two layouts: the layout of two phosphor sheets of yellow and green and the layout of two phosphor sheets of yellow and red

For our research, we utilized the WLED devices with nine inner chips of LED, which is displayed by Figure 1(a). The wattage of every chip in blue color is 1.16W, whose wavelength is 453 nm. Figure 1(b) details the LED optical parameters. For the task of finding the optimal concentration for  $\text{LaSiO}_3\text{Cl}:\text{Ce}^{3+},\text{Tb}^{3+}$  and  $\text{Ca}_5\text{B}_2\text{SiO}_{10}:\text{Eu}^{3+}$ , the GYC and RYC layouts (two phosphor sheets of yellow and green and two phosphor sheets of yellow and red respectively) are suggested. The GYC layout contains two sheets of phosphor that are positioned over the chips in blue color.  $\text{LaSiO}_3\text{Cl}:\text{Ce}^{3+},\text{Tb}^{3+}$  layer is placed on top of the sheet of  $\text{YAG}:\text{Ce}^{3+}$  phosphor in yellow color as displayed by Figure 1(c). The RYC layout contains two sheets of phosphor that are positioned over the chips in blue color. A sheet of  $\text{Ca}_5\text{B}_2\text{SiO}_{10}:\text{Eu}^{3+}$  is placed on top of the yellow phosphor

layer  $\text{YAG:Ce}^{3+}$  as displayed by Figure 1(d). We can utilize the said layouts and enhance the chromatic quality as well as the luminous flux for WLED devices. We could obtain such result when the dispersion along with the red, green illumination portions of the WLED devices are increased. Nevertheless, the  $\text{LaSiO}_3\text{Cl:Ce}^{3+}, \text{Tb}^{3+}$  and  $\text{Ca}_5\text{B}_2\text{SiO}_{10}:\text{Eu}^{3+}$  concentration are still required an appropriate modification.



Lead frame: 4.7 mm Jentech Size-S

LED chip: V45H

Die attach: Sumitomo 1295SA

Gold Wire: 1.0 mil

Phosphor: ITC NYAG4\_EL

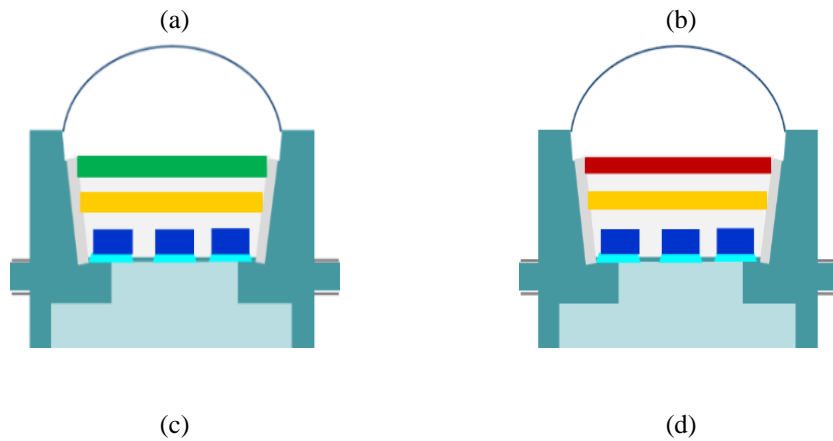


Figure 1. The MCW-LEDs with conversion phosphor: (a) The real MCW-LED device along with (b) its information; (c) GYC configuration (d) RYC configuration

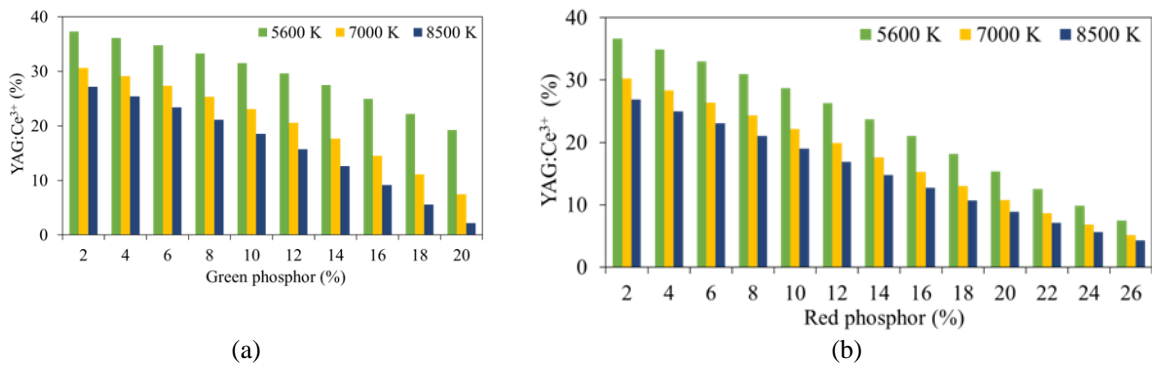


Figure 2. The concentration of phosphor in GYC (a) and RYC (b) fluctuates to sustain the standard CCTs

Figure 2 illustrates the contrasting alteration which occurs among the  $\text{LaSiO}_3\text{Cl:Ce}^{3+}, \text{Tb}^{3+}$  phosphor in green, the  $\text{Ca}_5\text{B}_2\text{SiO}_{10}:\text{Eu}^{3+}$  phosphor in red, and the  $\text{YAG:Ce}^{3+}$  phosphor in yellow. Such alteration serves two purposes: maintaining the mean CCTs, influencing the dispersion and absorption process in the two sheets of WLEDs, which guarantees a great impact to the hue standard and the illuminating beam in the WLED devices. When the concentration of  $\text{LaSiO}_3\text{Cl:Ce}^{3+}, \text{Tb}^{3+}$  and  $\text{Ca}_5\text{B}_2\text{SiO}_{10}:\text{Eu}^{3+}$  are increased from 2% to 20% wt as well as from 2% to 26% wt respectively, the yellow phosphor concentration declines so that the standard CCT levels can be sustained. Such condition applies to different WLED devices having various chromatic temperatures such as 6600 K and 7700 K.

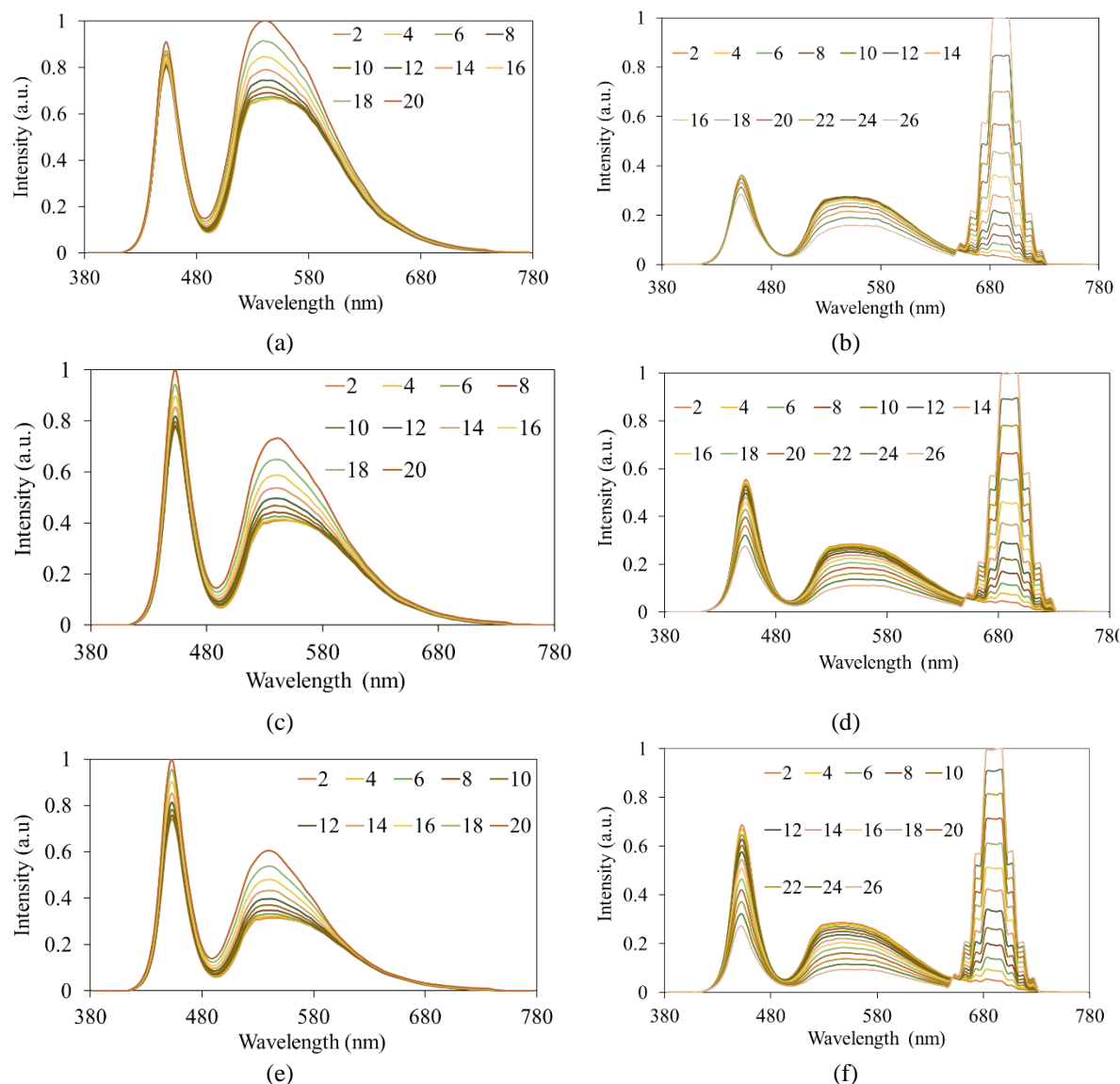


Figure 3. The emission spectrum in layouts of two phosphor sheets: (a) GYC - 5600 K; (b) RYC - 5600 K; (c) GYC - 7000 K; (d) RYC - 7000 K; (e) GYC - 8500 K; (f) RYC - 8500 K

In Figure 3, the red phosphor  $\text{Ca}_5\text{B}_2\text{SiO}_{10}:\text{Eu}^{3+}$  concentration has a big effect on the emission spectrum in WLEDs. Depending on the demand for production, we can choose which concentration will be used. WLEDs which require significant chromatic performance will have a minor decline of lumen output. The intensity in certain regions of the spectrum, 420 nm to 480 nm as well as 500 nm to 640 nm will rise along with the  $\text{LaSiO}_3\text{Cl}:\text{Ce}^{3+},\text{Tb}^{3+}$  concentration. Additionally, as the dispersion of blue illumination within the WLED device is increased, the dispersion within the phosphor sheet as well as within the WLED device will increase as well, this is advantageous for color uniformity. This is an important result when  $\text{LaSiO}_3\text{Cl}:\text{Ce}^{3+},\text{Tb}^{3+}$  is applied. Obviously, in the spectral region 649 nm – 738 nm, the intensity will rise with the  $\text{Ca}_5\text{B}_2\text{SiO}_{10}:\text{Eu}^{3+}$  concentration. The emission spectrum must be increased in two other regions (420 nm to 480 nm along with 500 nm to 600 nm). The boost in the 420 nm – 480 nm emission spectrum helps improve the lumen output for the dispersion of blue illumination. Greater chromatic temperature leads to greater spectrum, which means the chromatic efficiency and also the lumen output are higher. Although the modification of the chromatic efficiency in the WLED devices having significant temperature appear to be quite challenging, our research proves that  $\text{Ca}_5\text{B}_2\text{SiO}_{10}:\text{Eu}^{3+}$  can enhance the color quality in both low temperature (5600 K) and great temperature (8500 K).

### 3. RESULTS AND DISCUSSION

Light-emitting diodes create quasi-monochromatic illumination (i.e. with a limited emitting band), there are essentially two techniques to obtaining a white LED. For one side, a set of (at least) three LEDs with energy ratios tuned to produce white light with a given color temperature. A single LED, on the other side, may be utilized in conjunction with one or many phosphor materials to partly or completely transform the LED output.

The use of simply LEDs (no phosphor converters) provides some distinct advantages. To begin with, converting losses related to phosphor usage are eliminated. Moreover, it enables the construction of smart illuminations that may vary their emitting hue (from main hues to white light with changeable hue heating) and strength based on certain situations or the customer's preferences. Aside from ordinary lighting applications that merely require a constant hue and intensity, there is undoubtedly a significant market for these smart illumination types. LEDs' relatively narrow emission bands, along with the ability to select peak emission wavelengths, enable the production of light sources with a high LER and good color rendering. A 4-LEDs merge appears to be required for better color rendering. This will be quantified later. One drawback is that more complicated circuitry (perhaps with feedback mechanisms) must be utilized to compensate for the differential aging of current red, green, and blue LEDs. When frosting an RGB-LED combo when keeping the emitting hue, both current and temperature-dependent hue shifts are difficult. The spectrum shifts for these LEDs are generally not equal as a function of driving current and chip temperature related to the driving current, the ambient temperature as well as the apparatus' cooldown. Because smart LED-based illumination sources based on strength and hue selection, phosphor-free light sources need significant research work.

In contrast to the RGB technique, white light is generated via mixing a single LED illumination source with one or many converting phosphors. This method is currently used by the majority of commercially available LED-based white illumination sources. Until recently, these were nearly entirely based on a blue LED and a YAG:Ce<sup>3+</sup>-based phosphor. There are two techniques that may be distinguished. The first technique can utilize a blue LED and change a portion of the generated illumination into greater wavelengths by using a phosphor material, or another one can use phosphors to completely change the radiation from a (close)ultraviolet LED.

Owing to inherent 4f<sup>n</sup>–4f<sup>n</sup> transitions that are scarcely impacted by the host chemical, most trivalent rare-earth ions (with Ce<sup>3+</sup> being the notable exception) produce a set of rather strait emitting lines. However, the host determines the relative strength for the emission bands (through selecting standards related to local symmetry), the emission lines' cleavage related to the crystal field, as well as the quantum efficacy of these 4f–4f emitters (via the non-radiative pathways as well as the heat quenching behavior). Many of these rare-earth ions emit visible light. Tb<sup>3+</sup> (green radiation, main highest point at 545 nm) and Eu<sup>3+</sup> (orange to red radiation, the main highest point close to 600 or 620 nm) are particularly interesting rare-earth ions that have been thoroughly demonstrated to be beneficial in fluorescent light phosphors or cathode ray tubes. The main issue with shifting these substances to LED implementation, as previously stated, is the shortage of efficient, wide band stimulation routes in the close-UV to the blue proportion of the spectrum, as 5d levels and charge transfer states (CTS) are often located under 350 nm, as Y<sub>2</sub>O<sub>2</sub>S:Eu<sup>3+</sup>. Nevertheless, power shift from the MoO<sub>6</sub><sup>6-</sup> complex occurs in Eu<sup>3+</sup>-doped (Sr,Ba)<sub>2</sub>CaMoO<sub>6</sub>, allowing efficient pumping at 400 nm. By sensitizing with the right co-dopants, the stimulation spectrum can also be expanded to longer wavelengths. The extra of Ce<sup>3+</sup>, for example, can sensitize Tb<sup>3+</sup> emission. It has been reported that the addition of Bi<sup>3+</sup> creates additional (wide band) routes for Eu<sup>3+</sup>. We already mentioned that mixing thin line radiation at 460, 540, and 610 nm can result in efficient white light emission. In this instance, wLEDs with moderate hue rendering characteristics but great lighting effectiveness can be created. Surprisingly, the primary Tb<sup>3+</sup> and Eu<sup>3+</sup> emission peaks correspond to the requisite green and red components. Furthermore, the usage of Eu<sup>3+</sup>-doped red phosphors is favorable since the reabsorption of the green phosphor radiation is prevented, which may be an issue with red phosphors according to Eu<sup>2+</sup>.

The CRI parameter evaluates an entity's chroma as it is illuminated. The amount of excessive green illumination is the reason causing the chromatic disproportion among three key chromas, which include green, yellow and blue. This affects the chromatic efficiency in WLED devices which leads to the reduction of the chromatic fidelity in WLED devices. The result illustrated by Figure 3 (above) shows a slight decrease of CRI if the sheet of LaSiO<sub>3</sub>Cl:Ce<sup>3+</sup>,Tb<sup>3+</sup> phosphor is present, which is sufficient as the CRI parameter would merely be a CQS's facet. If compared, the CQS parameter is of greater importance while being more challenging to attain. Judging Figure 4, the CQS parameter remains the same as the concentration of LaSiO<sub>3</sub>Cl:Ce<sup>3+</sup>,Tb<sup>3+</sup> is under 8%. As such, 8% LaSiO<sub>3</sub>Cl:Ce<sup>3+</sup>,Tb<sup>3+</sup> concentration is applied, after considering the emission spectrum. Based on the result in Figure 3 (below), CRI rises with the concentration of Ca<sub>5</sub>B<sub>2</sub>SiO<sub>10</sub>:Eu<sup>3+</sup> at three mean CCT levels, which could be made clear via the absorption properties in the red phosphor layer. As Ca<sub>5</sub>B<sub>2</sub>SiO<sub>10</sub>:Eu<sup>3+</sup> absorbs the blue illumination produced by the LEDs chip, the granules of red phosphor change

the color of blue illumination into red. Besides,  $\text{Ca}_5\text{B}_2\text{SiO}_{10}:\text{Eu}^{3+}$  also absorbs the yellow illumination. Between the two absorptions, the absorption of the blue illumination generated by the chip in LED would be more potent, thanks to the material's absorption properties. The proportion of the red illumination of WLED devices is boosted if we additionally include  $\text{Ca}_5\text{B}_2\text{SiO}_{10}:\text{Eu}^{3+}$  which results in the rise of CRI. Judging the parameters of today's WLED device, CRI would be among the vital ones. Certainly, a bigger CRI results in a higher cost for making a WLED device. Regardless, the advantage offered by WLED with  $\text{Ca}_5\text{B}_2\text{SiO}_{10}:\text{Eu}^{3+}$  is the low price. For this reason, the  $\text{Ca}_5\text{B}_2\text{SiO}_{10}:\text{Eu}^{3+}$  can be widely used. However, the CRI would merely be an element intended for assessing chromatic performance for WLED devices. It does not mean that WLEDs with high CRI have high color quality. Therefore, modern studies have introduced another index which is CQS. CQS is a numeral figure which is defined by three elements: CRI, consumer interest, as well as chromatic coordinates. By including such elements, the CQS parameter is almost a general color quality scale. Figure 4 (below) demonstrates better CQS when the remote phosphor layer  $\text{Ca}_5\text{B}_2\text{SiO}_{10}:\text{Eu}^{3+}$  is increased. Plainly,  $\text{Ca}_5\text{B}_2\text{SiO}_{10}:\text{Eu}^{3+}$  can enhance the white-color quality for WLED devices with the two-layer phosphor arrangement. Such an outcome is vital for the research whose purpose involves boosting chromatic performance. We also must consider the impairment in the emission spectrum caused by the  $\text{Ca}_5\text{B}_2\text{SiO}_{10}:\text{Eu}^{3+}$  phosphor.

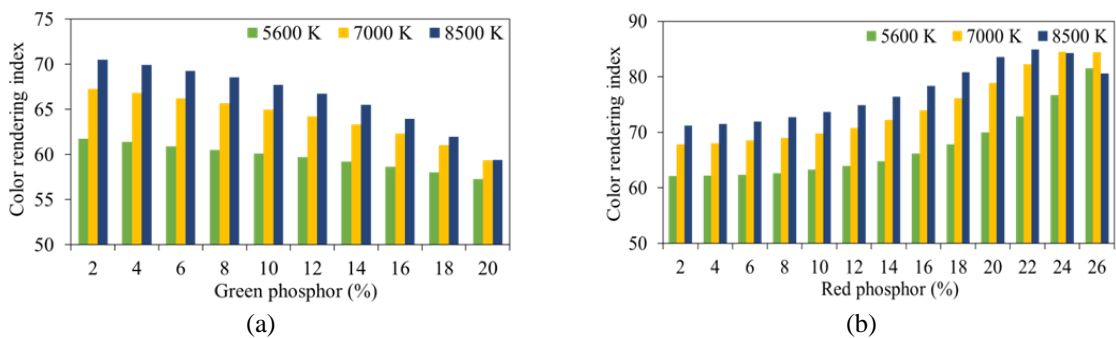


Figure 3. The CRI values with respective concentrations of  $\text{LaSiO}_3\text{Cl}:\text{Ce}^{3+}, \text{Tb}^{3+}$  and  $\text{Ca}_5\text{B}_2\text{SiO}_{10}:\text{Eu}^{3+}$ : (a) GYC; (b) RYC

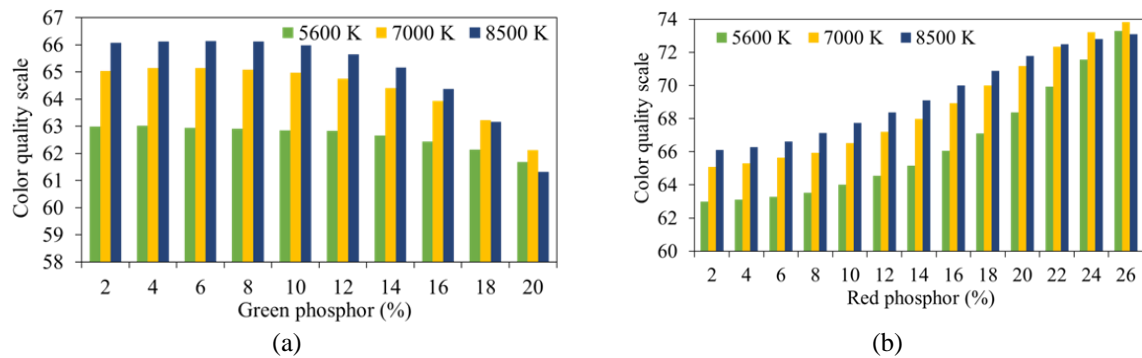


Figure 4. The CQS values with respective concentrations of  $\text{LaSiO}_3\text{Cl}:\text{Ce}^{3+}, \text{Tb}^{3+}$  and  $\text{Ca}_5\text{B}_2\text{SiO}_{10}:\text{Eu}^{3+}$ : GYC (a); RYC (b)

The mathematical configuration of the emitted blue illumination along with transformed yellow illumination in the dual-sheet phosphor arrangement, which could produce some significant change of LED efficiency can be attained, will be illustrated in this part. The emitted blue illumination along with the transformed yellow illumination packed in one-sheet remote phosphor having the phosphor layer's thickness of  $2h$ :

$$PB_I = PB_o \times e^{-2\alpha_{B1}h} \tag{1}$$

$$PY_I = \frac{1 \beta_1 \times PB_o}{2 \alpha_{B1} - \alpha_{Y1}} (e^{-2\alpha_{Y1}h} - e^{-2\alpha_{B1}h}) \tag{2}$$

The emitted blue illumination and transformed yellow illumination for dual-sheet distant phosphor layout having the phosphor layer's thickness of  $h$  which is as follow:

$$PB_2 = PB_0 \times e^{-2\alpha_{B1}h} \quad (3)$$

$$PY_2 = \frac{1}{2} \frac{\beta_2 \times PB_0}{\alpha_{B2} - \alpha_{Y2}} (e^{-2\alpha_{Y2}h} - e^{-2\alpha_{B2}h}) \quad (4)$$

Each phosphor sheet's thickness is represented by  $h$ . The one-sheet and dual-sheet distant phosphor packages are respectively displayed via the subscripts "1" and "2".  $\beta$  represents the converting factor when the blue illumination transforms into yellow. The yellow illumination's reflecting factor is represented by  $\gamma$ . The light intensity for the blue LED device is the blue illumination's (also known as PB) and the yellow light's (also known as PY) intensity which would be illustrated by  $PB_0$ . The ratios of the wasted power for blue and yellow illuminations throughout their circulation within the sheet of phosphor are depicted as  $\alpha_B$ ;  $\alpha_Y$  accordingly. The dual-layer phosphor arrangement significantly improves the illumination effectiveness of pc-LEDs if compared to the one-sheet counterpart:

$$\frac{(PB_2 + PY_2) - (PB_1 + PY_1)}{PB_1 + PY_1} > 0 \quad (5)$$

The theory of Mie-scattering [20-23] is utilized so that we could analyze the dispersion among  $Ca_5B_2SiO_{10}:Eu^{3+}$  particle. The said theory is used in the following expression to calculate the cross-section scattering  $C_{sca}$  in globular granules. The law of Lambert-Beer [24-26] computes the converted light power as below:

$$I = I_0 \exp(-\mu_{ext}L) \quad (6)$$

For the above equation, the incident light power is indicated by  $I_0$ , the phosphor layer thick is  $L$  (determined by mm), with the extinction coefficient indicated by  $\mu_{ext}$ . It is also illustrated as  $\mu_{ext} = N_r C_{ext}$ , with  $N_r$  being the amount of density of particle distribution ( $mm^{-3}$ ) and  $C_{ext}$  ( $mm^2$ ) describes the extinction cross-section of phosphor.

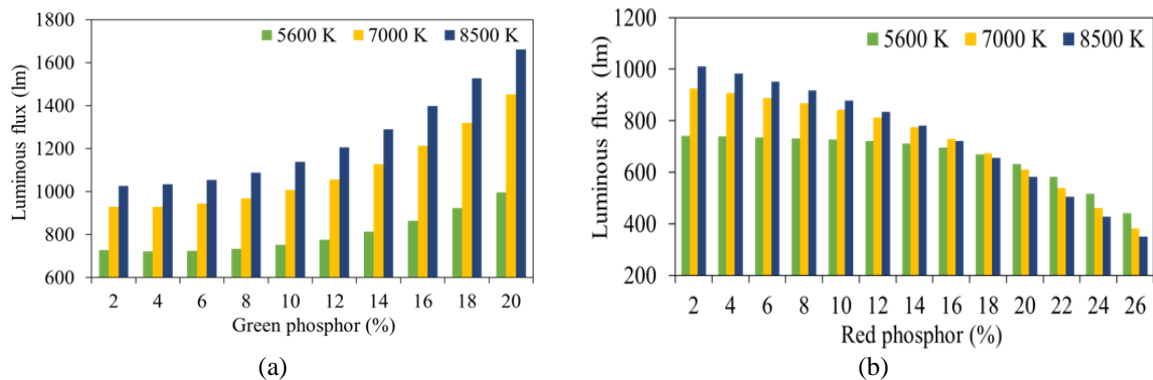


Figure 5. The lumen values with respective concentrations of  $LaSiO_3Cl:Ce^{3+}, Tb^{3+}$  and  $Ca_5B_2SiO_{10}:Eu^{3+}$ : (above) GYC; (below) RYC

From the algebraic expression (5), the luminous efficacy in the WLED devices having dual-sheet remote phosphor structure appear to be higher compared to the efficacy in the one-sheet structure. Certainly, our research proves the emission spectrum's effectiveness in the two-sheet remote phosphor structure. Figure 5 (as shown) emphasizes a considerable escalation of the emission spectrum as  $LaSiO_3Cl:Ce^{3+}, Tb^{3+}$  concentration is increased from 2% wt. to 20% wt. But the lumen output in the two-sheet remote phosphor would be significantly affected by the concentration of the  $Ca_5B_2SiO_{10}:Eu^{3+}$  phosphor sheet. When we apply the Lambert-Beer law, apparently, the decreasing coefficient  $\mu_{ext}$  would be directly proportional to the  $Ca_5B_2SiO_{10}:Eu^{3+}$  while being inversely proportional to the power of optical propagation. Therefore, when maintaining the thickness for two sheets of phosphor of the WLED devices, the emission spectrum could be diminished as the  $Ca_5B_2SiO_{10}:Eu^{3+}$  concentration increases. In fact, Figure 5 shows the reduction of the lumen output at five CCT levels. As the concentration of  $Ca_5B_2SiO_{10}:Eu^{3+}$  reaches 26% wt., the lumen output reduces remarkably. But if we include the advantage offered by the red phosphor  $Ca_5B_2SiO_{10}:Eu^{3+}$  to augment the CRI and the CQS, along with the advantage that the two-sheet remote phosphor layout offers over the one-sheet phosphor one (not having a sheet of phosphor in red), the reduction could be totally tolerable. One final issue



would be that the manufacturers must adopt an acceptable concentration of  $\text{Ca}_5\text{B}_2\text{SiO}_{10}:\text{Eu}^{3+}$  that is suitable in WLEDs mass production.

#### 4. CONCLUSION

This paper illustrates how the green phosphor  $\text{LaSiO}_3\text{Cl}:\text{Ce}^{3+},\text{Tb}^{3+}$  along with the red phosphor  $\text{Ca}_5\text{B}_2\text{SiO}_{10}:\text{Eu}^{3+}$  would influence the CRI, CQS parameters as well as the lumen output in the two-sheet phosphor structure. Using the theory of Mie-scattering and the law of Beer–Lambert, our study proves that  $\text{Ca}_5\text{B}_2\text{SiO}_{10}:\text{Eu}^{3+}$  is the most suitable phosphor intended for boosting the chromatic performance. In addition,  $\text{LaSiO}_3\text{Cl}:\text{Ce}^{3+},\text{Tb}^{3+}$  phosphor would be used for boosting the luminous performance of WLEDs. This would be accurate for the WLEDs in small temperature (6600 K) as well as in high temperature (8500 K). Therefore, the outcome of our research would meet the goal to enhance the chromatic performance of the white illumination which would be very hard to complete with the remote phosphor arrangement. Nevertheless, there are still some downsides happen to the emission spectrum. When the concentration of  $\text{LaSiO}_3\text{Cl}:\text{Ce}^{3+},\text{Tb}^{3+}$  and  $\text{Ca}_5\text{B}_2\text{SiO}_{10}:\text{Eu}^{3+}$  reached more than the allowed amount, the chromatic performance and the luminous flux will decline remarkably. This is the reason why it is crucial to adopt a suitable concentration based on the production target. This research provides many pieces of key information as references for the better manufacture of WLEDs.

#### ACKNOWLEDGEMENTS

This study was financially supported by Van Lang University, Vietnam.

#### REFERENCES

- [1] L. Xiao, C. Zhang, P. Zhong, and G. He, "Spectral optimization of phosphor-coated white LED for road lighting based on the mesopic limited luminous efficacy and IES color fidelity index," *Appl. Opt.*, vol. 57, pp. 931-936, 2018.
- [2] L. Li, *et al.*, "On the  $\text{Er}^{3+}$  NIR photoluminescence at 800 nm," *Opt. Express*, vol. 28, pp. 3995-4000, 2020, doi: 10.1364/AO.57.000931.
- [3] G. Zhang, G. He, and M. Zhang, "Spectral optimization of color temperature tunable white LEDs with red LEDs instead of phosphor for an excellent IES color fidelity index," *OSA Continuum*, vol. 2, pp. 1056-1064, 2019, doi: 10.1364/OE.20.00A684.
- [4] McDonnell, E. Coyne, and G. M. O'Connor, "Grey-scale silicon diffractive optics for selective laser ablation of thin conductive films," *Appl. Opt.*, vol. 57, pp. 6966-6970, 2018, doi: 10.1364/AO.57.006966.
- [5] P. Zhu, H. Zhu, S. Thapa, and G. C. Adhikari, "Design rules for white light emitters with high light extraction efficiency," *Opt. Express*, vol. 27, pp. A1297-A1307, 2019, doi: 10.1364/oe.27.0a1297.
- [6] H. Lee, H. Cho, C. W. Byun, J. H. Han, B. H. Kwon, S. Choi, J. Lee, and N. S. Cho, "Color-tunable organic light-emitting diodes with vertically stacked blue, green, and red colors for lighting and display applications," *Opt. Express*, vol. 26, pp. 18351-18361, 2018, doi: 10.1364/OE.26.018351.
- [7] X. Yang, X. Yang, C. Chai, J. Chen, S. Zheng, and C. Chen, "Single 395 nm excitation warm WLED with a luminous efficiency of 104.86 lm/W and a color rendering index of 90.7," *Opt. Mater. Express*, vol. 9, pp. 4273-4286, 2019, doi: 10.1364/ome.9.004273.
- [8] H. Kim, Y. J. Seo, B. Yang, and H. Y. Chu, "Transparent effect on the gray scale perception of a transparent OLED display," *Opt. Express*, vol. 26, pp. 4075-4084, 2018, doi: 10.1364/OE.25.003954.
- [9] X. Fu, P. Lu, J. Zhang, Z. Qu, W. Zhang, Y. Li, P. Hu, W. Yan, W. Ni, D. Liu, and J. Zhang, "Micromachined extrinsic Fabry-Pérot cavity for low-frequency acoustic wave sensing," *Opt. Express*, vol. 27, pp. 24300-24310, 2019, doi: 10.1364/OE.27.024300.
- [10] X. Li, D. Kundaliya, Z. J. Tan, M. Anc, and N. X. Fang, "Projection lithography patterned high-resolution quantum dots/thiol-ene photo-polymer pixels for color down conversion," *Opt. Express*, vol. 27, pp. 30864-30874, 2019, doi: 10.1364/OE.27.030864.
- [11] Y. T. Wang, C. W. Liu, P. Y. Chen, R. N. Wu, C. C. Ni, C. J. Cai, Y. W. Kiang, and C. C. Yang, "Color conversion efficiency enhancement of colloidal quantum dot through its linkage with synthesized metal nanoparticle on a blue light-emitting diode," *Opt. Lett.*, vol. 44, pp. 5691-5694, 2019, doi: 10.1364/OL.44.005691.
- [12] X. Leng, W. Chapman, B. Rao, S. Nandy, R. Chen, R. Rais, I. Gonzalez, Q. Zhou, D. Chatterjee, M. Mutch, and Q. Zhu, "Feasibility of co-registered ultrasound and acoustic-resolution photoacoustic imaging of human colorectal cancer," *Biomed. Opt. Express*, vol. 9, pp. 5159-5172, 2018, doi: 10.1364/BOE.9.005159.
- [13] H. Lin, A. Verma, C. Y. Kang, Y. M. Pai, T. Y. Chen, J. J. Yang, C. W. Sher, Y. Z. Yang, P. T. Lee, C. C. Lin, Y. C. Wu, S. K. Sharma, T. Wu, S. R. Chung, and H. C. Kuo, "Hybrid-type white LEDs based on inorganic halide perovskite QDs: candidates for wide color gamut display backlights," *Photon. Res.*, vol. 7, pp. 579-585, 2019, doi: 10.1364/PRJ.7.000579.
- [14] Y. Zhang, J. Wang, W. Zhang, S. Chen, and L. Chen, "LED-based visible light communication for color image and audio transmission utilizing orbital angular momentum superposition modes," *Opt. Express*, vol. 26, pp. 17300-17311, 2018, doi: 10.1364/OE.26.017300.
- [15] G. Prabhakar, P. Gregg, L. Rishoj, P. Kristensen, and S. Ramachandran, "Octave-wide supercontinuum generation of light-carrying orbital angular momentum," *Opt. Express*, vol. 27, pp. 11547-11556, 2019, doi: 10.1364/OE.27.011547.




- [16] S. P. Groth, A. G. Polimeridis, A. Tambova, and J. K. White, "Circulant preconditioning in the volume integral equation method for silicon photonics," *J. Opt. Soc. Am. A*, vol. 36, pp. 1079-1088, 2019, doi: 10.1364/JOSAA.36.001079.
- [17] J. H. Kim, B. Y. Kim, and H. Yang, "Synthesis of Mn-doped CuGaS<sub>2</sub> quantum dots and their application as single downconverters for high-color rendering solid-state lighting devices," *Opt. Mater. Express*, vol. 8, pp. 221-230, 2018, doi: 10.1364/OME.8.000221.
- [18] X. Yuan, M. Zhao, X. Guo, Y. Li, Y. Yu, Z. Gan, and H. Ruan, "Ultra-high capacity for three-dimensional optical data storage inside transparent fluorescent tape," *Opt. Lett.*, vol. 45, pp. 1535-1538, 2020, doi: 10.1364/OL.387278.
- [19] Z. Li, Y. Tang, J. Li, X. Ding, C. Yan, and B. Yu, "Effect of flip-chip height on the optical performance of conformal white-light-emitting diodes," *Opt. Lett.*, vol. 43, pp. 1015-1018, 2018, doi: 10.1364/OL.43.001015.
- [20] P. J. Pardo, M. I. Suero, and Á. L. Pérez, "Correlation between perception of color, shadows, and surface textures and the realism of a scene in virtual reality," *J. Opt. Soc. Am. A*, vol. 35, pp. B130-B135, 2018, doi: 10.1364/JOSAA.35.00B130.
- [21] Bai, J. Qian, S. Dang, T. Peng, J. Min, M. Lei, D. Dan, and B. Yao, "Full-color optically-sectioned imaging by wide-field microscopy via deep-learning," *Biomed. Opt. Express*, vol. 11, pp. 2619-2632, 2020, doi: 10.1364/BOE.389852.
- [22] Polzer, S. Ness, M. Mohseni, T. Kellerer, M. Hilleringmann, J. Rädler, and T. Hellerer, "Correlative two-color two-photon, 2C2P. excitation STED microscopy," *Biomed. Opt. Express*, vol. 10, pp. 4516-4530, 2019, doi: 10.1364/BOE.10.004516.
- [23] Y. Xie, Y. Yu, J. Gong, C. Yang, P. Zeng, Y. Dong, B. Yang, R. Liang, Q. Ou, and S. Zhang, "Encapsulated room-temperature synthesized CsPbX<sub>3</sub> perovskite quantum dots with high stability and wide color gamut for display," *Opt. Mater. Express*, vol. 8, pp. 3494-3505, 2018, doi: 10.1364/OME.8.003494.
- [24] Motazedifard, S. Dehbod, and A. Salehpour, "Measurement of thickness of thin film by fitting to the intensity profile of Fresnel diffraction from a nanophase step," *J. Opt. Soc. Am. A*, vol. 35, pp. 2010-2019, 2018, doi: 10.1364/JOSAA.35.002010.
- [25] Y. Zhou, Y. Wei, F. Hu, J. Hu, Y. Zhao, J. Zhang, F. Jiang, and N. Chi, "Comparison of nonlinear equalizers for high-speed visible light communication utilizing silicon substrate phosphorescent white LED," *Opt. Express*, vol. 28, pp. 2302-2316, 2020, doi: 10.1364/OE.383775.
- [26] W. Liu, L. Jiang, W. Han, J. Hu, X. Li, J. Huang, S. Zhan, and Y. Lu, "Manipulation of LIPSS orientation on silicon surfaces using orthogonally polarized femtosecond laser double-pulse trains," *Opt. Express*, vol. 27, pp. 9782-9793, 2019, doi: 10.1364/OE.27.009782.

## BIOGRAPHIES OF AUTHORS



**Dieu An Nguyen Thi** received a master of Electrical Engineering, HCMC University of Technology and Education, VietNam. Currently, she is a lecturer at the Faculty of Electrical Engineering Technology, Industrial University of Ho Chi Minh City, Viet Nam. Her research interests are Theoretical Physics and Mathematical Physics. She can be contacted at email: nguyenthidieuan@iuh.edu.vn.  
 ORCID: 0000-0002-5327-1002  
 Scopus: Dieu An Nguyen nguyenthidieuan@iuh.edu.vn.  
 Google Scholar: [https://scholar.google.com/citations?view\\_op=list\\_works&hl=vi&user=qNwCM0oAAAAJ](https://scholar.google.com/citations?view_op=list_works&hl=vi&user=qNwCM0oAAAAJ)  
 Publons: <https://publons.com/researcher/4954208/nguyen-thi-dieu-an/>



**Phan Xuan Le**    received a Ph.D. in Mechanical and Electrical Engineering from Kunming University of Science and Technology, Kunming city, Yunnan province, China. Currently, He is a lecturer at the Faculty of Engineering, Van Lang University, Ho Chi Minh City, Viet Nam. His research interests are Optoelectronics(LED), Power transmission and Automation equipment. He can be contacted at email: le.px@vlu.edu.vn  
 Scopus: Le Phan Xuan phanxuanle.ts@gmail.com

ID Google scholar:

<https://scholar.google.com.vn/citations?hl=vi&user=e6QPpLEAAAAJ>

The scopus id:

<https://www.scopus.com/authid/detail.uri?authorId=57200312062>